

Novel Routes to Cu(salicylaldimine) Covalently Bound to Silica: Combined Pulse EPR and in Situ Attenuated Total Reflection-IR Studies of the Immobilization

Eamonn F. Murphy,[†] Davide Ferri,[‡] and Alfons Baiker*

Laboratory of Technical Chemistry, Swiss Federal Institute of Technology, ETH Hönggerberg-HCI, CH-8093 Zurich, Switzerland

Sabine Van Doorslaer[§] and Arthur Schweiger*

Laboratory of Physical Chemistry, Swiss Federal Institute of Technology, ETH Hönggerberg-HCI, CH-8093 Zurich, Switzerland

Received April 29, 2002

Several novel routes for the immobilization of modified Cu(salicylaldimine) complexes on commercially available silica are described. New pulse electron paramagnetic resonance (EPR) and electron-nuclear double resonance sequences, which provide more detailed information than that available previously, in combination with continuous wave EPR, allow a definitive assignment of the geometry at the copper center in the immobilized Cu(salicylaldimine). Immobilization of the modified Cu(salicylaldimine) on silica was followed in situ by monitoring the intensity of the characteristic free- and metal-coordinated imine bands as a function of time using attenuated total reflectance IR spectroscopy. On the basis of these studies, the outcome of the Schiff base condensation of Cu-bis(salicylaldehyde) with γ -aminopropyl-modified silica gel is shown to provide immobilized *trans*-O₂N₂- and O₃N-coordinated immobilized Cu(salicylaldimine)-type compounds. In addition, *trans*-O₂N₂- or O₃N-coordinated copper centers are selectively prepared on silica by controlling the aminopropyl modifier loading, thus opening a route to compounds not available by conventional synthesis. The O₃N-coordinated Cu(salicylaldimine)-type compound on silica was investigated as a precursor for the synthesis of a tethered chiral Cu(salicylaldimine) via reaction of the coordinated carbonyl group with (*R*)-(+)- α -methylbenzylamine. Supported Cu(salicylaldimine) was also prepared via the immobilization of the appropriate silylethoxy-modified homogeneous precursor on silica gel. Precursors and silica-supported Cu(salicylaldimine) materials have been fully characterized. Comparisons are drawn with related Cu(salicylaldimine) immobilized in silica aerogels.

Introduction

In the present contribution, we exploit one of the oldest chemical reactions known, the Schiff base condensation,¹ for the immobilization of Cu(salicylaldimine) systems on silica.

* Authors to whom correspondence should be addressed. Telephone: +41 1 632 31 53 (A.B.); +41 1 632 43 62 (A.S.), Fax: +41 1 632 11 63 (A.B.); +41 1 632 10 21 (A.S.). E-mail: baiker@tech.chem.ethz.ch (A.B.); schweiger@esr.phys.chem.ethz.ch (A.S.).

[†] Present address: Analytical Services, CarboGen Laboratories (Aarau) AG, Schachenallee 29, CH-5001 Aarau, Switzerland.

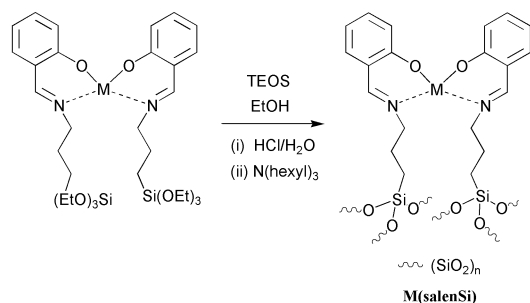
[‡] Present address: Bruker Optics GmbH, Industriestrasse 26, CH-8117 Fällanden, Switzerland.

[§] Present address: Spectroscopy in Biophysics and Catalysis (SIBAC) Laboratory, University of Antwerp, Universiteitsplein 1, B-2610 Wilrijk, Belgium.

(1) Schiff, H. *Ann. Suppl.* **1864**, 3, 343.

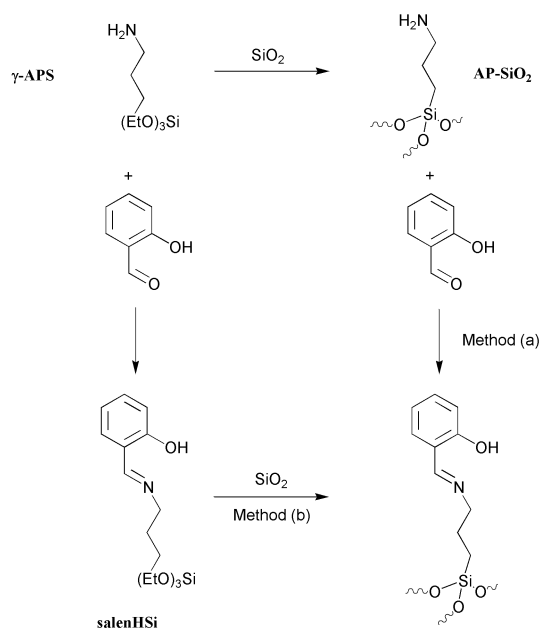
The application of novel pulse electron paramagnetic resonance (EPR) and electron-nuclear double resonance (ENDOR) techniques allows the coordination geometry at the copper center on the surface to be defined. Using attenuated total reflectance infrared spectroscopy (ATR-IRS), we monitor in situ the immobilization process. A recent review article confirms the relevance of such N-containing ligand systems in homogeneous and heterogeneous catalysis.² Salicylaldimine [*N,N'*-ethylenebis(salicylidenaminato)] compounds of the first-row transition metals, an important subgroup of this class, have been extensively investigated

(2) Fache, F.; Schulz, E.; Tommasino, M. L.; Lemaire, M. *Chem. Rev.* **2000**, *100*, 2159.

Scheme 1. Sol-gel Immobilization of M(salenSi)-Type Compounds in Silica-Aerogel Matrices (M = Cu, Co)

as models for enzymes that reversibly bind di-oxygen and, consequently, have found use in catalysis.^{3–8} Given the technical advantages of working with heterogeneous systems in catalysis, numerous approaches have been exploited to immobilize the aforementioned compounds.^{9–12} Encapsulation based on steric restraints in porous materials such as zeolites, providing the so-called ship-in-a-bottle materials, has found wide application and has naturally been extended to the preparation of immobilized chiral M(salicylaldimine).¹³ Organic-polymer-supported M(salicylaldimine), prepared by the copolymerization of the ligand and a monomer link, suffers the intrinsic problem of poor stability of the hydrocarbon backbone under the harsh reaction conditions often necessary for di-oxygen activation.¹² Silica, on the other hand, is a readily available support combining relatively “inert” properties with good mechanical stability.¹⁴ Recently, some of us have demonstrated that M(salenSi)-type compounds (salenSi = silyloxy-modified salicylaldimine) can be incorporated in silica aero- and xerogels via the *sol-gel* method, followed by the supercritical extraction of the *wet* gels (Scheme 1).¹⁵ In the adoption of this approach, the metal–ligand system is covalently bound to the silica surface, thus allowing flexibility in engineering the pore structure and surface area of the support.¹⁶

Given the remarkable stability of the silica–aerogel-incorporated Co(salenSi) under oxidizing conditions,¹⁵ we set out to further investigate these systems from a synthetic standpoint and characterize them in greater detail. In the present work, the Schiff base reactions investigated fall into

Scheme 2. Preparation and Immobilization Routes of salenHSi

two groups (Schemes 2 and 3): (i) reactions of silica-immobilized γ -aminopropyl groups (AP-SiO₂) with aldehydes and M-bis(salicylaldehyde) and (ii) reactions of γ -(aminopropyl)ethoxysilane with aldehydes, providing modified homogeneous precursor ligands and complexes. Surface modifications with a propyl phosphine,¹⁷ sulfide,¹⁸ and amine¹⁹ function pervade the literature with applications ranging from the removal of contaminants from wastewater to the modification of titania–silica aerogels for base-catalyzed epoxidation.²⁰ Numerous examples can be found of AP-SiO₂ where the metal center of the catalyst is axially coordinated, or *anchored*, via the Lewis base nitrogen of the immobilized aminopropyl group.^{21,22} Another pertinent application of this amine–aldehyde condensation is found in the preparation of homogeneous chiral “salen” compounds, where the chiral center is introduced via the condensation of a primary amine with a M-bis(salicylaldehyde).^{23–28} In the present contribution, the Schiff base condensation of γ -(aminopropyl)triethoxysilane (γ -APS) with salicylaldehyde and Cu-bis(salicylaldehyde) (**1**) is exploited in the preparation of silica-immobilized Cu(salenSi). Although preliminary

- (3) McLendon, G.; Martell, A. E. *Coord. Chem. Rev.* **1976**, *19*, 1.
- (4) Niederhoffer, E. C.; Tommsons, J. H.; Martell, A. E. *Chem. Rev.* **1984**, *84*, 137.
- (5) Jones, R. D.; Summerville, D. A.; Basolo, F. *Chem. Rev.* **1979**, *79*, 139.
- (6) Smith, T. D. *Coord. Chem. Rev.* **1981**, *39*, 295.
- (7) Jacobsen, E. N. In *Catalytic Asymmetric Synthesis*; Ojima, I., Ed.; VCH: New York, 1993.
- (8) Jacobsen, E. N. In *Comprehensive Organometallic Chemistry II*; Abel, E. W., Stone, F. G. A., Wilkinson, G., Eds.; Pergamon: New York, 1995; Vol. 12.
- (9) Bhadbhade, M. M.; Srinivas, D. *Inorg. Chem.* **1993**, *32*, 6122.
- (10) Deshpande, S.; Srinivas, D.; Ratsanamy, P. *J. Catal.* **1999**, *188*, 261.
- (11) Koner, S. *Chem. Commun.* **1998**, 593.
- (12) Drago, R. S.; Gaul, J.; Zombeck, A.; Straab, D. K. *J. Am. Chem. Soc.* **1980**, *102*, 1033.
- (13) Canali, L.; Sherrington, D. C. *Chem. Soc. Rev.* **1999**, *28*, 85.
- (14) Price, P. M.; Clark, J. H.; Macquarrie, D. J. *J. Chem. Soc., Dalton Trans.* **2000**, 101.
- (15) Murphy, E. F.; Schmid, L.; Bürgi, T.; Maciejewski, M.; Baiker, A.; Günther, D.; Schneider, M. *Chem. Mater.* **2001**, *13*, 1296.
- (16) Huesing, N.; Schuber, U. *Angew. Chem., Int. Ed.* **1998**, *37*, 22.

- (17) Shyu, S. G.; Cheng, S. W.; Tzou, D. L. *Chem. Commun.* **1999**, 2337.
- (18) Liu, M.; Hidajat, K.; Kawi, S.; Zhao, D. Y. *Chem. Commun.* **2000**, 1145.
- (19) Feng, X.; Ryxell, G. E.; Wang, L. Q.; Kim, A. Y.; Liu, J.; Kemner, K. M. *Science* **1997**, *276*, 923.
- (20) Müller, C.; Schneider, M. A.; Mallat, T.; Baiker, A. *J. Catal.* **2000**, *192*, 448.
- (21) Liu, C. J.; Li, S. G.; Pang, W. Q.; Che, C. M. *Chem. Commun.* **1997**, 65.
- (22) Zhou, X. G.; Yu, X. Q.; Huang, J. S.; Li, S. G.; Che, C. M. *Chem. Commun.* **1999**, 1789.
- (23) Talzi, E. P.; Nekipelov, V. M.; Zamaraev, K. I. *Russ. J. Phys. Chem.* **1984**, *58*, 273.
- (24) Harada, K.; Shiono, K.; Nomoto, S. *Chem. Lett.* **1980**, 1271.
- (25) McKenzie, E. D.; Selvey, S. J. *Inorg. Chim. Acta* **1985**, *101*, 127.
- (26) Joesten, M. D.; Krasney, E. L.; Neidert, J. B. *Inorg. Chim. Acta* **1989**, *159*, 143.
- (27) Sacconi, L.; Ciampolini, M.; Maggio, F.; Del Re, G. *J. Am. Chem. Soc.* **1960**, *82*, 815.
- (28) Ray, P.; Mukherjee, A. K. *J. Indian Chem. Soc.* **1950**, *27*, 707.

reports of the immobilization of related M(salenSi)-type compounds^{15,29,30} and the stepwise synthesis of a chiral Mn(salicylaldimine) have appeared,³¹ to our knowledge the latter approach has not been described to date.

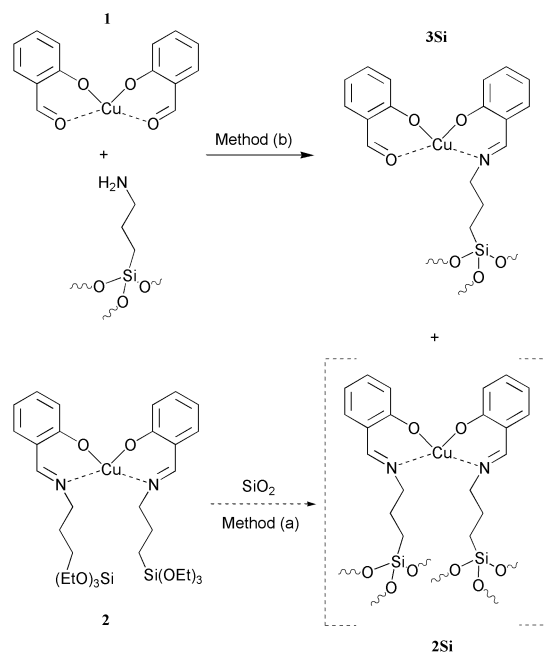
In the past, an overwhelming dearth of convincing evidence for the structure assignments of immobilized complexes has permeated the literature, and the complete characterization of the immobilized species has often been substituted by speculation based on IR data.^{29–31} In addition to the standard spectroscopic methods, novel pulse EPR techniques^{32,33} are utilized here to provide definitive assignments of the metal coordination geometry on silica. Cu(II) compounds are ideal candidates for EPR studies, and we show here that continuous wave (CW) EPR, in combination with advanced pulse EPR and ENDOR techniques, can be used to identify the coordination geometry at the metal center on the surface. The versatility of ATR-IRS for monitoring processes occurring at solid–liquid interfaces is well-established. A salient feature of this method is that it allows the detection of (sub)monolayers of molecules lying at the surface even in the presence of a strongly absorbing medium (e.g., solvent).³⁴ In the present study, ATR-IRS is used to follow the in situ stepwise immobilization of Cu(salenSi) on silica gel. The synthetic strategy for Cu(salenSi) immobilization and a complete characterization of the immobilized complex are the focus of this work.

Experimental Section

Materials and Methods. All solvents and chemicals were supplied by Fluka and used without further purification. Silica gel 100 was purchased from Merck.

AP-SiO₂ Gel. Silica gel with various aminopropyl loadings was prepared according to the literature method.³⁵ Dimethylamino-propyl-modified silica with a loading of about 1.00 mmol g⁻¹ silica used in isophorone isomerization studies was prepared using an identical procedure.³⁶ **1**, shown in Scheme 3, was prepared according to the literature procedures.^{37,38} Elemental analyses (CHN) were performed in-house. The metal content of the silica gels was determined by inductively coupled plasma atomic emission spectroscopy. Fourier transform infrared (FTIR) spectra were recorded as KBr pellets or neat thin-liquid films using a Bruker IFS-66/S instrument. NMR spectra were run on a Bruker 300-MHz spectrometer. The specific surface areas (*S*_{BET}), mean cylindrical pore diameters (*d*_p), and specific desorption pore volumes (*V*_{PN2}) were determined by nitrogen physisorption at 77 K using a Micrometrics ASAP 2000 instrument. X-ray photoelectron spectroscopy (XPS) measurements were performed on a Leybold Heraeus LHS11 apparatus using Mg K α radiation. The spectrometer energy scale

Scheme 3. Immobilization of **1** on AP-SiO₂ and Modified Homogeneous Cu(salenSi) Precursors



was calibrated using the Au *f*_{7/2}, Ag 3*d*_{5/2}, and Cu 2*p*_{3/2} lines at 84.2, 367.9, and 932.4 eV. Thin sample films were pressed on a steel holder for analysis. Slight sample charging was compensated for by using the C 1*s* line at 284.8 eV as an internal standard. Quantification was performed using the sensitivity factors according to Wagner et al.³⁹ Thermal analyses were carried out on a Netzsch STA 409 thermoanalyzer connected via a heated (ca. 200 °C) stainless-steel capillary to a Balzers quadrupole mass spectrometer QMG 420.

CW EPR. CW EPR spectra were recorded at room temperature and 120 K on a Bruker ESP300 spectrometer (microwave frequency of 9.43 GHz), equipped with a liquid-nitrogen cryostat. A microwave power of 20 mW, a modulation amplitude of 0.5 mT, and a modulation frequency of 100 kHz were used.

Pulse EPR and ENDOR Spectroscopy. The X-band pulse EPR and ENDOR spectra were recorded at 10 K on a Bruker Elexsys spectrometer (microwave frequency of 9.69 GHz) equipped with a liquid-helium cryostat from Oxford Inc. The magnetic field was measured with a Bruker ER 035M NMR gaussmeter. In all pulse EPR and ENDOR experiments, a repetition rate of 1 kHz was used.

Davies ENDOR.⁴⁰ The pulse sequence $\pi-T-\pi/2-\tau-\pi-\tau$ -echo, with a selective radio-frequency π pulse of variable frequency ν_{rf} applied during time *T*, was used. To detect the strongly (weakly) coupled nuclei, the following pulse lengths and time intervals were used: $t_{\pi} = 48$ (200) ns, $t_{\pi/2} = 24$ (100) ns, $t_{\tau}^{rf} = 15$ μ s, $\tau = 400$ ns, and *T* = 17 μ s.

Hyperfine Sublevel Correlation (HYSCORE).⁴¹ The experiments were carried out with the pulse sequence $\pi/2-\tau-\pi/2-t_1-\pi-t_2-\pi/2-\tau$ -echo with pulse lengths $t_{\pi/2} = 24$ ns and $t_{\pi} = 16$ ns and an interpulse delay $\tau = 128$ ns. The time intervals *t*₁ and *t*₂ were varied from 96 to 6496 ns in steps of 16 ns. An eight-step phase cycle was used to eliminate unwanted echoes. The time traces of the HYSCORE spectra were baseline-corrected with a third-

(29) Chisem, J. S.; Rafelt, J.; Shieh, M. T.; Chisem, J.; Clark, J. H.; Jachuck, R.; Macquarrie, D.; Ramshaw, C.; Scott, K. *Chem. Commun.* **1998**, 1949.

(30) Feng, H. X.; Wang, R. M.; He, Y. F.; Lei, Z. Q.; Wang, Y. P.; Xia, C. G.; Suo, J. S. *J. Mol. Catal. A: Chem.* **2000**, *159*, 25.

(31) Kim, G. J.; Shin, J. H. *Catal. Lett.* **1999**, *63*, 205.

(32) Schweiger, A.; Jeschke, G. *Principles of Pulse Electron Paramagnetic Resonance*; Oxford University Press: Oxford, U.K., 2001.

(33) Van Doorslaer, S.; Schweiger, A. *Naturwissenschaften* **2000**, *87*, 245.

(34) Harrick, N. J. *Internal Reflection Spectroscopy*; Interscience Publishers: New York, 1967.

(35) Bolm, D.; Fey, T. *Chem. Commun.* **1999**, 1795.

(36) Murphy, E. F.; Baiker, A. *J. Mol. Catal. A: Chem.* **2002**, *179*, 233.

(37) Tyson, G. N.; Adams, S. C. *J. Am. Chem. Soc.* **1940**, *62*, 1228.

(38) Pfeiffer, P.; Breith, E.; Luebbe, E.; Tsumaki, T. *Liebigs Ann. Chem.* **1933**, *503*, 84.

(39) Wagner, C. D.; Davis, L. E.; Zeller, M. V.; Taylor, J. A.; Raymond, R. M.; Gale, L. H. *Surf. Interface Anal.* **1981**, *3*, 211.

(40) Davies, E. R. *Phys. Lett. A* **1974**, *47*, 1.

(41) Höfer, P.; Grupp, A.; Nebenführ, H.; Mehring, M. *Chem. Phys. Lett.* **1986**, *132*, 279.

order polynomial, apodized with a Hamming window, and zero-filled. After two-dimensional Fourier transformation, the absolute-value spectra were calculated. All simulations were made using the EasySpin program, a MATLAB toolbox developed for EPR and ENDOR simulations (see <http://www.esr.ethz.ch>).

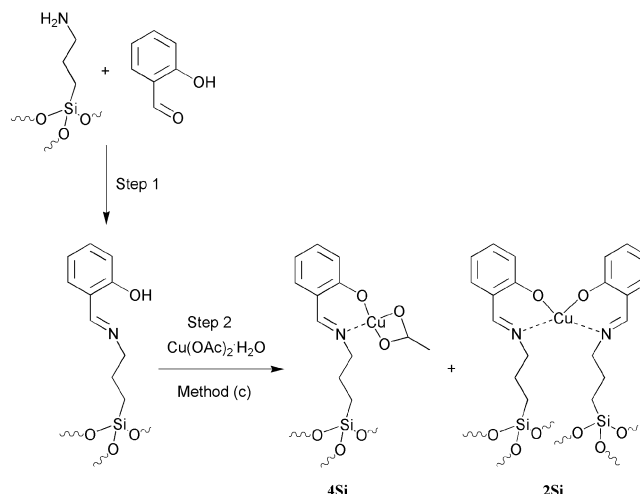
In Situ ATR-IRS. In situ ATR-IR experiments were performed at ambient temperature using a purpose-built stainless-steel flow cell and commercial ATR unit (Wilks Scientific) as described elsewhere⁴² together with a $52 \times 20 \times 2$ mm trapezoidal KRS-5 internal reflection element (IRE; Graseby Specac), affording eight active reflections. ATR spectra were recorded by accumulating 200 scans at a 4-cm^{-1} resolution at an angle of incidence of 45° on a Bruker IFS 66/S spectrometer equipped with a liquid-nitrogen-cooled medium-band MCT detector. The AP-SiO₂ films were prepared according to a modification of the method described by McQuillan and co-workers.⁴³ Typically, a carbon tetrachloride suspension of the silica sample was sonicated for 30 min, pipetted onto the IRE, and air-dried. After gentle washing with carbon tetrachloride, the amount of deposited material remaining corresponded to about 1.0–1.5 mg. The air-dried, coated IRE was directly mounted in the wall of the flow cell. Following the stabilization of the IR signal with neat ethanol flowing over the silica (ca. 2 h), solutions of salicylaldehyde and, subsequently, copper acetate in ethanol (10 mM) were introduced over the AP-SiO₂ film. Spectra are presented in absorbance units with the final spectrum recorded during neat-ethanol flow, which served as the reference.

Synthetic Procedures. salenHSi. Solutions of salenHSi were prepared (Scheme 2) by the addition of an equimolar amount of γ -APS (1.77 g, 8 mmol) in ethanol (30 mL) to a stirred ethanolic (20 mL) solution of salicylaldehyde (0.98 g, 8 mmol). The resulting bright-yellow solution was stirred at room temperature for a further 2 h. Removal of solvent at 40 °C under vacuum afforded a bright-yellow liquid. Decomposition and partial condensation were observed on heating the liquid to high temperatures, and, therefore, the crude product was characterized and used without distillation. Yield: 2.42 g (93%). IR (neat): 2974, 2927, 2886, 1634, 1615, 1583, 1498, 1462, 1443, 1414, 1390, 1343, 1281, 1186, 1166, 1152, 1103, 1080, 958, 896, 793, 757, 737 cm^{-1} . ¹H NMR (CDCl₃): 13.6 (1H, s, OH), 8.32 (1H, s, HCN), 7.28 (1H, m, aromatic), 7.23 (1H, m, aromatic), 6.95 (1H, m, aromatic), 6.85 (1H, m, aromatic), 3.82 (6H, q, CH₃CH₂O), 3.58 (2H, m, NCH₂, propyl), 1.82 (2H, m, CH₂, propyl), 1.22 (9H, t, CH₃CH₂O), 0.68 (2H, m, CH₂Si). ¹³C NMR (CDCl₃): 164.9 (CN), 161.6 (COH), 132.2 (Ar), 131.3 (Ar), 119 (Ar), 118.6 (Ar), 117.2 (Ar), 62.2 (NCH₂, propyl), 58.6 (CH₂, ethoxy), 24.6 (CH₂, propyl), 18.5 (CH₃, ethoxy), 8.2 (SiCH₂, propyl).

Cu(salenSi) Precursor 2. The preparation and full characterization of the Cu(salenSi) precursor **2** have been described previously.¹⁵ Alternatively, **2** has been prepared via the reaction of **1** with 2 equiv of γ -APS in ethanol. IR and elemental analyses are identical with those previously described.¹⁵ Reactions of **1** with 1 equiv of γ -APS gave a mixture of **2** and unreacted **1**.

salenHSi Immobilization on Silica. Method a. Salicylaldehyde (0.61 g, 5 mmol) in ethanol (10 mL) was added dropwise to a suspension of AP-SiO₂ (2.00 g, modifier 1.00 mmol g⁻¹) in ethanol (25 mL) and stirred at room temperature for 8 h. The solid product was recovered by filtration, washed with copious amounts of ethanol, and dried in vacuo at 80 °C for 24 h (Scheme 2). An IR

Scheme 4. Reaction of Copper Acetate with salenHSi-Modified Silica Providing **4Si** and **2Si** at Low (0.05 mmol g⁻¹) and High (0.50 mmol g⁻¹) Modifier Loading, Respectively



spectrum of the product is shown in Figure 6. Found (theory for C₂₀H₂₄N₂O₇Si₃₅ ca. 1.00 mmol g⁻¹ silica): C, 9.21 (9.77); N, 1.02 (1.14). Found (theory for C₁₀H₁₂NO₇Si₃₄ ca. 0.50 mmol g⁻¹ silica): C, 4.95 (5.41); N 0.52 (0.63). Found (theory for C₁₀H₁₂NO₆₆₄Si₃₃₁ ca. 0.05 mmol g⁻¹ silica): C, 0.52 (0.60); N, 0.04 (0.07).

Method b. Under argon, a solution of salenHSi (8 mmol) in ethanol (30 mL) was added dropwise to a suspension of silica (6.00 g) in ethanol (30 mL) and stirred at room temperature for 8 h. The product was recovered and characterized as described above.

Cu(salenSi) 2 on Silica (2Si). Method a: Homogeneous Cu(salenSi) Precursor plus Silica. Silica gel was added to an ethanolic solution (50 mL) of the appropriate Cu(salenSi) precursor (4 mmol) under argon and stirred for 18 h at room temperature (Scheme 3). Higher Cu(salenSi) loadings are achieved at higher reaction temperatures and by increasing the reaction time. The silica-immobilized Cu(salenSi) was filtered off in air, washed with ethanol until the washings were clear, and, finally, washed with acetone. The solid was dried in vacuo at 80 °C for 8 h.

2Si. Green-brown color. IR (KBr): 3023, 2972, 2923, 1625, 1539, 1469, 1450, 910, 755, 736 cm^{-1} . Found (theory for CuN₂C₂₀H₂₂Si₆₂O₁₂₈·25H₂O): C, 4.97 (5.17); H, 8.93 (11.32); N, 0.48 (0.60); Cu, 1.29 (1.37). XPS for the **2Si** sample gives atomic ratios for Cu (1), N (2.1), Si (62), C (128), and O (61) that are in good agreement with the elemental analysis.

Method b: Reaction of 1 with AP-SiO₂. A solution of **1** (0.31 g, 1 mmol) in dimethyl sulfoxide (DMSO; 30 mL) was added to a suspension of AP-SiO₂ (1.00 g, modifier 1 mmol g⁻¹ silica) in DMSO (20 mL) and stirred at room temperature under argon for 24 h (Scheme 3). The silica-immobilized **2Si** was recovered and washed with copious amounts of DMSO and acetone until the washings were clear.

Method c: Stepwise Buildup of 2Si on Silica. Copper acetate hydrate (0.20 g, 1 mmol) in DMSO (20 mL) was added to a suspension of the immobilized salenHSi (1.00 g, modifier 1 mmol g⁻¹ silica) in DMSO (30 mL) under argon (Scheme 4). The suspension was stirred for 24 h at room temperature and the solid product recovered as described in method b.

3 on Silica (3Si). **1** (0.15 g, 0.5 mmol) in DMSO (30 mL) was added to a DMSO (40 mL) suspension of AP-SiO₂ (2.00 g, modifier 0.05 mmol g⁻¹ silica) under argon and stirred for 18 h at room temperature (Scheme 3). The pale-green product was collected by filtration in air and washed with DMSO until the washings were clear, followed by acetone. The solid was dried at 80 °C for 6 h in

(42) Ferri, D.; Bürgi, T.; Baiker, A. *J. Phys. Chem. B* **2001**, *105*, 3187.

(43) Connor, P. A.; Dobson, K. D.; McQuillan, A. *J. Langmuir* **1995**, *11*, 4193.

vacuo. IR (KBr): 2928, 1629, 1548, 1527, 1473, 1448, 1427, 1415, 1404, 971, 955, 801, 750, 713, 470 cm^{-1} . Found (theory for $\text{C}_{17}\text{H}_{16}\text{-NCuO}_{666}\text{Si}_{331}$ ca. 0.05 mmol g^{-1} silica): C, 0.83 (1.01); N, 0.04 (0.07).

4Si. A DMSO solution (30 mL) of copper acetate (0.040 g, 0.2 mmol) was added to a DMSO (40 mL) suspension of salenHSi-modified silica (2.00 g, modifier 0.05 mmol g^{-1} silica) under argon and stirred for 18 h at room temperature (Scheme 4). The pale-green product was collected by filtration in air and washed with DMSO until the washings were clear, followed by acetone. The solid was dried at 80 °C for 6 h in vacuo. IR (KBr, cm^{-1}): see Figure 6. Found (theory for $\text{C}_{12}\text{H}_{14}\text{NCuO}_{666}\text{Si}_{331}$ ca. 0.05 mmol g^{-1} silica): C, 0.55 (0.71); N, 0.04 (0.07).

Reaction of 1 with (R)-(+)- α -Methylbenzylamine (α -MBA) To Give 5. **1** (0.22 g, 0.72 mmol) was suspended in ethanol (15 mL) and stirred under argon. The suspension gives way to a dark-brown solution on addition of α -MBA (0.26 g, 2.15 mmol) under N_2 . The solution was heated to reflux for 3 h and allowed to cool to room temperature, and the volume was reduced to 1 mL. Addition of pentane gave a dark-brown precipitate, which was filtered off, washed with pentane/acetone, and dried in vacuo at 60 °C for 8 h. Yield: 0.11 g (23%). Mp: 142–144 °C. Found (theory for $\text{C}_{30}\text{H}_{26}\text{N}_2\text{O}_2\text{Cu}$): C, 70.39 (70.64); H, 5.26 (5.14); N, 5.44 (5.49). IR (KBr): 1627, 1617, 1598, 1538, 1496, 1472, 1448, 1409, 1396, 1342, 1327, 1200, 1148, 1077, 926, 889, 770, 755, 702 cm^{-1} .

Test Reaction of α -MBA with 3Si. **3Si** (1.00 g, modifier 0.05 mmol g^{-1} silica) was treated with α -MBA (0.12 g, 1 mmol) in ethanol at 70 °C for 5 h under argon. The solid product was recovered by filtration, washed with ethanol, and dried at 60 °C in vacuo for 8 h. IR spectra of the recovered and starting material were similar, probably due to low aminopropyl modifier on silica, which makes it difficult to detect change. The outcome of the reaction was, therefore, determined by EPR as described in the Results section.

Results

This section begins with a description of the ligands used for immobilization. To present the results of metal-complex immobilization in a coherent form, the spectroscopic studies and synthetic approach are presented together here and discussed separately in the Discussion section.

(A) salenHSi with Pendant Propylsilylethoxy Groups; Soluble Precursors and in Situ Synthesis on AP-SiO₂. The salenHSi used for immobilization on silica is characterized in detail for the first time. The ligand is readily prepared via the reaction of γ -APS with salicylaldehyde (Scheme 2) and forms almost instantaneously at room temperature. Strong intramolecular hydrogen bonding in salenHSi (δ 13.6) gives rise to a large downfield shift of the hydroxyl proton resonance.⁴⁴ In addition, the six-membered rings formed via hydrogen bonding are probably stabilized by the conjugated double-bond systems, leading to lower than normally expected frequencies for these double-bond vibrations. Following immobilization on silica, hydrogen bonding to the hydroxy groups on the surface, as in the ring conformation adopted by the propylamine group on silica, is expected.^{43,45,46}

Table 1. Physical and Textural Properties of Silica-Immobilized Intermediates and Copper Compounds Formed during the Stepwise Synthetic Procedure

sample	S_{BET} ($\text{m}^2 \text{g}^{-1}$)	V_{pN_2} ($\text{cm}^3 \text{g}^{-1}$)	d_p (nm)
SiO_2^a	354	0.91	8.8
AP-SiO ₂ (1 mmol g^{-1})	299	0.78	8.7
salenHSi on SiO ₂ (1 mmol g^{-1})	276	0.65	8.3
4 on SiO ₂ (0.05 mmol g^{-1})	294	0.64	7.8
2 on SiO ₂ (1 mmol g^{-1})	291	0.63	7.8

^a As supplied by Merck.

Immobilization of the aminopropyl modifier and salenHSi on silica involves stirring solutions of the silylethoxy-modified ligands with silica in a dry solvent (Scheme 2). The influence of water in the solvent and moist air during curing and calcining on the outcome of the immobilization of γ -APS have been studied extensively using various spectroscopic techniques.^{45,46} Dichloromethane was chosen as the solvent here to minimize the co-condensation of two or more (aminopropyl)silanes in solution during immobilization.⁴⁷ Under these conditions, the γ -APS groups condense predominantly with Si-OH groups, or physisorbed water molecules on the silica surface, leading to immobilization. Thermogravimetric analysis of the silica, as supplied by Merck, established that about 1.2% by wt corresponded to physisorbed water. Alternatively, silica-immobilized salenHSi is available via surface synthesis involving the direct reaction of AP-SiO₂ with salicylaldehyde (Scheme 2).

Thermal treatment of the AP-SiO₂ gel determines the conformation adopted by the aminopropyl group on the surface and the degree of condensation of the silylethoxy groups.^{45,46} Condensation of γ -APS is almost quantitative in the vacuum-dried (80 °C, 8 h) modified silica as determined by thermogravimetric analysis. The degree of condensation in Cu- and Co(salenSi) silica aerogels was also determined in an analogous way by the quantitative measurement of ethanol evolution from the modified silica as a function of temperature.¹⁵ Alternatively, ²⁹Si NMR has been employed to quantify the different silicon centers present.⁴⁸ The position of the NH₂ deformation band in the IR spectrum of the silica-immobilized γ -APS (ca. 1600 cm^{-1}) suggests that a closed ring conformation is adopted by the modifier on the surface in the absence of any solvent, that is, H-bonding of the amino group with surface OH groups.^{45,46} Approximating the area occupied by one aminopropyl group to be 40 Å would imply that with 1 mmol of aminopropyl modifier *per* 1.00 g silica, about 70% of the available surface area is covered (Table 1). Modification of the silica surface does not influence the pore volume and surface area significantly (Table 1). In contrast for AP-SiO₂ aerogels, the physical and textural properties of the material depend heavily on reaction parameters including the base amount and time of addition.^{16,49}

(B) Model EPR Studies of 1. CW EPR has been used extensively to study Cu(II) complexes.³² Consequently,

(44) Percy, G. C.; Thornton, D. A. *J. Inorg. Nucl. Chem.* **1972**, *34*, 3369.

(45) Vrancken, K. C.; van der Voort, P.; Gillis-D'Hamera, I.; Vansant, E. F. *J. Chem. Soc., Faraday Trans.* **1992**, *88*, 3197.

(46) De Haan, J. W.; van den Bogaert, H. M.; Ponjee, J. J. *J. Colloid Interface Sci.* **1986**, *110*, 591.

(47) Chiang, C. H.; Ishida, H.; Koenig, J. I. *J. Colloid Interface Sci.* **1980**, *74*, 396.

(48) Schmid, L.; Kröcher, O.; Köppel, R. A.; Baiker, A. *Microporous Mesoporous Mater.* **2000**, *35–36*, 181.

(49) Schneider, M.; Baiker, A. *Catal. Rev.—Sci. Eng.* **1995**, *37*, 515.

Table 2. g and Copper Hyperfine^a Values for **1** in Different Matrices

compound	component	matrix	$g_{\parallel} \pm$ 0.005	$ A_{\parallel} \pm$ 10 MHz	$g_{\perp} \pm$ 0.015	$ A_{\perp} \pm$ 20 MHz
1 ·H ₂ O or 1 ·MeOH	1	MeOH/H ₂ O	2.315	450	2.065	80
1 ·DMSO	2	DMSO	2.359	420	2.080	40
1 ·H ₂ O	3	DMSO	2.320	440	2.065	40
1 on SiO ₂	4	silica	2.359	420	2.080	40
	5	silica	2.295	520	2.070	40

^a The hyperfine values are given for the ⁶³Cu isotope.

extensive literature compilations are available, and a comparison of the measured EPR parameters with these facilitates classification of the immobilized complex under study. Our discussion is confined to type-2 complexes, which are largely square-planar with a possible fifth weak coordination site. Type-2 copper complexes are characterized by a nearly axial g matrix and a resolved hyperfine coupling in the parallel direction ($|A_{\parallel}| > 400$ MHz) for which g_{\parallel} and A_{\parallel} correlate with the type of equatorial coordination atoms.⁵⁰ Because the g_{\parallel} and A_{\parallel} values also depend on the charge of the surrounding ligands and a possible fifth ligand, a definitive determination of the coordination sphere based on CW EPR alone is not possible. A preliminary investigation of **1** in different solvents is used here to evaluate which EPR and ENDOR techniques are appropriate for the further characterization of immobilized copper complexes.

The CW EPR parameters obtained from a frozen solution of **1** in methanol/water (1:1; component 1) and DMSO (components 2 and 3) are collected in Table 2. Because the EPR parameters of component 3 are similar to those of 1, it is likely that the spectrum of 3 arises from **1** with an axial water ligand. Possible structures for component 2 are **1** with or without the axial ligation of DMSO. The former is unlikely since g_{\parallel} (component 2) $>$ g_{\parallel} (component 3), and it is known that g_{\parallel} increases for copper Schiff bases upon axial ligation. Talzi et al. found $g_{\parallel} = 2.262$ for **1** in chloroform, which is clearly lower than the g_{\parallel} values observed here.⁵¹ Finally, the $|A_{\parallel}|$ values of components 1–3 fall in the range reported for **1**·L, where L is a weak or strong base in trans configuration (trans, 420–500 MHz; cis, 508–555 MHz).⁵¹ It should be noted that **1** may adopt a trans or cis arrangement of the ligands relative to the copper center. Thus far, we have described only *trans*-**1**, which might be expected on the basis of reducing the steric interactions of the aromatic rings of the salicylaldehyde groups.

During the immobilization experiments, **1** was observed to adsorb on the silica surface. The CW EPR spectrum of adsorbed **1** has two components (Table 2). Component 4 is similar to 2, whereas component 5 is very similar to that reported for the cis form of **1**·MeOH. This indicates that in both cases axial ligation is taking place and most likely coordination to OH groups on the surface or solvent molecules is involved.

For a more detailed characterization, X-band ENDOR and ESEEM (electron spin echo envelope modulation) experi-

ments were conducted on frozen methanol/water and DMSO solutions of **1**. The ENDOR technique allows investigation of the interactions of the unpaired electron at the paramagnetic center with the surrounding protons and strongly coupled nitrogens equatorially bound to Cu(II). Weakly coupled nitrogens, such as those of axial nitrogen bases, cannot be observed with ENDOR. Conversely, weakly coupled nitrogens as well as ¹³C and ²⁹Si nuclei (in natural abundance) can be studied with ESEEM spectroscopy. The ENDOR spectrum of an $S = 1/2$, $I = 1/2$ system (e.g., an unpaired electron coupled to a ¹H nucleus) consists of two peaks at frequencies $\nu_{\alpha,\beta} = |a/2 \pm \nu_1|$, where a is the hyperfine value at the given observer position and ν_1 is the nuclear Zeeman frequency that is characteristic for each nucleus. In the case of *weak* coupling ($|a/2| < |\nu_1|$), the signals are centered around the nuclear Zeeman frequency; in the *strong*-coupling case, the signals are centered around $a/2$. Figure 1 shows the Davies-ENDOR spectra taken as a function of the magnetic field for the frozen methanol/water solution of **1**. The signals are all centered around the proton Zeeman frequency (ν_{H}) and can, therefore, be ascribed to proton interactions. The spectra were recorded using strong and short microwave pulses (48/24/48 ns), which suppress the ENDOR signals of the weakly coupled protons (central signals marked by *).^{52,53} Parts b and e of Figure 1 show the slices at the observer positions B and A indicated in part a. The corresponding simulations for the largest proton hyperfine interaction are shown in parts c and f of Figure 1. The simulation parameters are $A_1 = 18.8$ MHz, $A_2 = 14.4$ MHz, and $A_3 = 14.0$ MHz, whereby the A_3 axis lies along g_{\parallel} . The hyperfine values lie between those found for the aldehydic proton of Cu-bis(salicylaldoximate) ($A_1 = 13$ MHz, $A_2 = 9.15$ MHz, and $A_3 = 8.48$ MHz)⁵⁴ and Cu[*N,N'*-ethylenebis(salicylidenaminato)] ($A_1 = 22.8$ MHz, $A_2 = 19.38$ MHz, and $A_3 = 18.43$ MHz).⁵⁵ The ENDOR signals can, therefore, be ascribed to the aldehyde protons of the salicylaldehyde ligand. In parts d and g of Figure 1, the corresponding ENDOR spectra taken of **1** in dry DMSO at observer positions B and A are shown. It becomes clear that although the g and copper hyperfine values depend strongly on the matrix (compare data of components 1 and 2 in Table 2), the hyperfine values of the aldehyde protons are independent of the matrix. Consequently, this coupling may be used as a marker for the presence of the salicylaldehyde ligand.

Figure 2 shows the Davies-ENDOR spectra obtained with weak and long microwave pulses (200/100/200 ns) for **1** in frozen methanol/water (parts a and c) and dry DMSO (parts b and d). The use of weak microwave pulses avoids the suppression of the weakly coupled protons (region marked with * in Figure 1a). It is clear that the ENDOR spectra of **1** in DMSO lack some of the proton signals present in the ENDOR spectra of **1** in methanol/water (arrows in parts a and c of Figure 2; maximum coupling around 6 MHz). These signals evidently stem from the protons of the axially

(50) Peisach, J.; Blumberg, W. E. *Arch. Biochem. Biophys.* **1974**, *165*, 691.

(51) Talzi, E. P.; Nekipelov, V. M.; Zamaraev, K. I. *Russ. J. Phys. Chem.* **1984**, *58*, 165.

(52) Thomann, H.; Bernardo, M. *Methods Enzymol.* **1993**, *227*, 118.

(53) Gemperle, C.; Schweiger, A. *Chem. Rev.* **1991**, *91*, 1481.

(54) Schweiger, A.; Günthard, H. H. *Chem. Phys.* **1978**, *32*, 35.

(55) Kita, M.; Hashimoto, M.; Iwazumi, M. *Inorg. Chem.* **1979**, *18*, 3432.

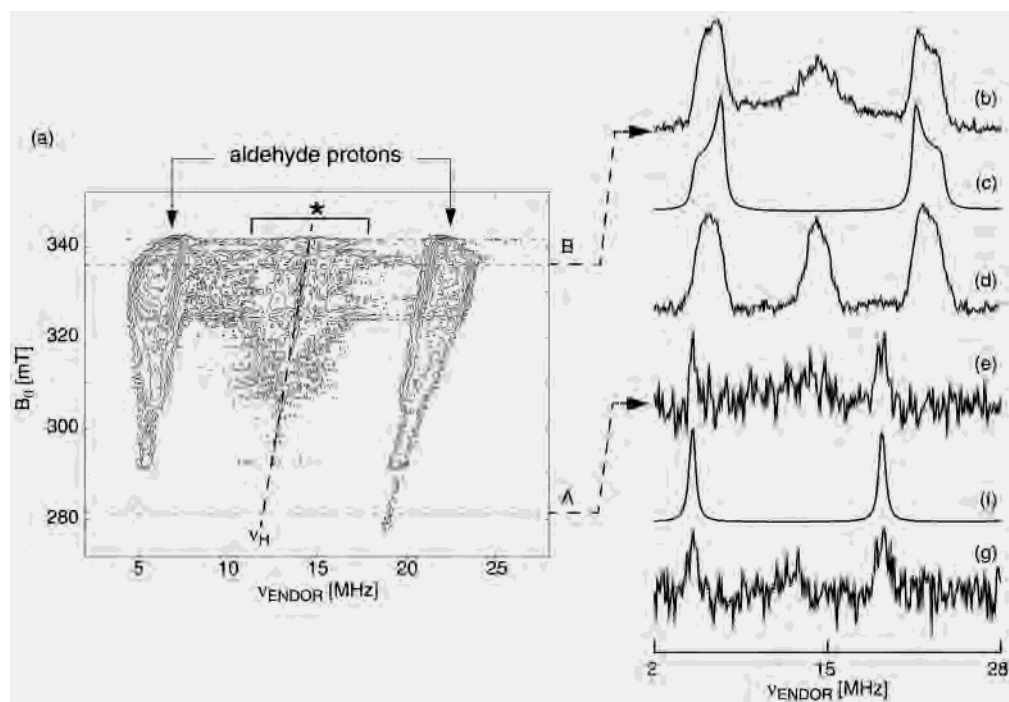


Figure 1. Davies-ENDOR spectra (hard and short microwave pulses). (a) **1** in methanol/water as a function of the magnetic field. (b) Observer position B in part a ($B_0 = 336$ mT). (c) Simulation of part b. (d) **1** in DMSO at observer position B. (e) Observer position A in part a ($B_0 = 281$ mT). (f) Simulation of part e. (g) **1** in DMSO at observer position A.

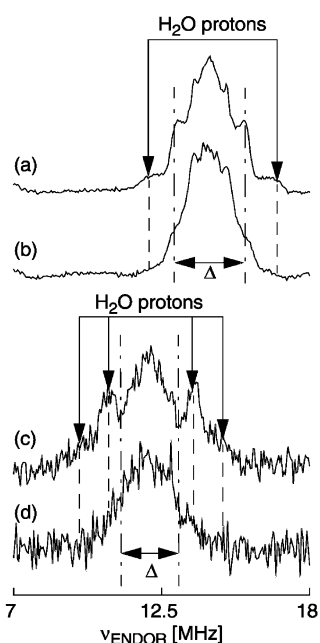


Figure 2. Davies-ENDOR spectra (weak and long pulses). **1** in (a) methanol/water and (b) DMSO, both at observer position B (see Figure 1a). **1** in (c) methanol/water and (d) DMSO at observer position A (see Figure 1a).

coordinated water or methanol molecule. The observed maximum coupling is slightly lower than that observed for the hyperfine coupling of the axial water protons in the copper hexa-aquo complex.⁵⁶ The signals in the region marked by Δ arise predominantly from interactions with the benzyl protons. Splittings of up to 1.9 MHz have been observed for the benzyl protons in Cu-bis(salicylaldoximate)

and are slightly smaller than the maximum splittings observed here (around 2.5 MHz).⁵⁴ The remaining differences between the ENDOR spectra in both solvents can be ascribed to the proton signals of the methyl protons of DMSO, which are missing in the case of methanol/water.

The HYSORE spectrum of **1** in methanol/water taken at observer position B ($B_0 \parallel g_{\perp}$) is shown in Figure 3a. HYSORE allows for a correlation between the nuclear frequencies of the two m_S manifolds. The interpretation of the HYSORE spectra of disordered systems has been discussed by several authors.^{57–59} Here, we confine ourselves to a qualitative discussion of the spectra. The HYSORE spectrum in Figure 3a shows interactions with the ^1H and ^{13}C nuclei. The ridges at about 5.22 and 22.5 MHz correspond to the aldehyde proton observed at these frequencies in the Davies-ENDOR spectrum (Figure 1). Furthermore, the cross peaks of the axial water protons can be observed. The fact that these ridges are not parallel to the antidiagonal at ν_H implies a significant anisotropy of the hyperfine interaction.⁵⁷ This is again in accordance with the observations for the axial water protons in the Cu(II) hexa-aquo complex.⁵⁶ Finally, a ridge stemming from the hyperfine interaction with the ^{13}C nuclei of the salicylaldehyde ligands is observed. This ridge can again be used as a marker for the presence of the ligand.

(C) Immobilization Procedures with EPR and ENDOR Analyses of Immobilized Cu(salenSi) Compounds. The synthetic procedures developed for immobilization of

(56) Atherton, N. M.; Horsewill, A. J. *J. Mol. Phys.* **1979**, *37*, 1349.

(57) Pöpl, A.; Kevan, L. *J. Phys. Chem.* **1996**, *100*, 3387.

(58) Dikanov, S. A.; Bowman, M. K. *J. Magn. Reson., Ser. A* **1995**, *116*, 125.

(59) Dikanov, S. A.; Xun, L.; Karpel, A. B.; Tyryshkin, A. M.; Bowman, M. K. *J. Am. Chem. Soc.* **1996**, *118*, 8408.

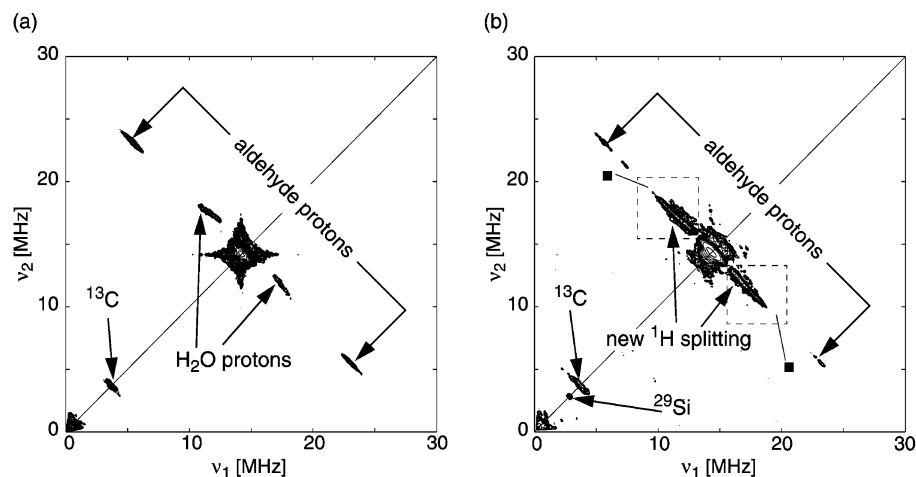


Figure 3. HYSORE spectra. (a) **1** in methanol/water and (b) immobilized mixture of **2Si** and **3Si** (sample D), both at observer position B (see Figure 1a).

Table 3. g and Copper Hyperfine^a Values for the Different Immobilized Copper Compounds on Silica

sample	compound	relative amount (%)	$g_{ } \pm 0.005$	$ A_{ } \pm$		geometry
				10 MHz	$g_{\perp} \pm 0.015$	
A ^b	3Si	50	2.285	465	2.065	NO ₃
	2Si	50	2.230	500	2.065	N ₂ O ₂
B ^c	3Si	100	2.290	465	2.065	NO ₃
C ^d	2Si	100	2.243	550	2.065	N ₂ O ₂
D ^e	3Si	52	2.283	470	2.065	NO ₃
	2Si	48	2.237	515	2.065	N ₂ O ₂
E ^f	4Si	88	2.288	450	2.065	NO ₃
	Cu(OAc) ₂ /SiO ₂	12	2.360	420	2.065	O ₄
F ^g	3Si + α -MBA	100	2.283	470	2.065	NO ₃
G ^h	Cu(OAc) ₂ /SiO ₂	100	2.360	420	2.068	O ₄

^a The hyperfine values are given for the ⁶³Cu isotope. ^b A = 1 + AP-SiO₂ at intermediate modifier loading (0.50 mmol g⁻¹). ^c B = 1 + AP-SiO₂ at low modifier loading (0.05 mmol g⁻¹). ^d C = A after catalytic run. ^e D = 1 + 1 equiv γ -APS and immobilization on silica. ^f E = copper acetate + salenHSiO₂ (0.50 mmol g⁻¹). ^g F = B + α -MBA. ^h G = copper acetate adsorbed on silica.

Cu(salenSi) complexes are summarized in Scheme 3. Our new approach for the immobilization of Cu(salenSi) involves the smooth Schiff base condensation of the copper-coordinated aldehyde groups of readily available **1** with aminopropyl groups covalently bound to silica (Scheme 3). Copper hyperfine couplings and g values for the different compounds immobilized on silica and copper acetate directly interacting with silica are listed in Table 3. The CW EPR spectra of the reaction products of **1** with AP-SiO₂ are depicted in Figure 4. The type of product(s) on the surface following immobilization is strongly dependent on the aminopropyl modifier loading on the silica (Scheme 3), as shown by EPR. For the intermediate-loading case (sample A, Table 3) two components are observed. The decrease in $g_{||}$ and the increase in $|A_{||}|$ observed for the first versus the second component (Table 3) are typical for a larger involvement of nitrogen atoms in the direct coordination of Cu(II).⁵⁰ Talzi et al. reported $g_{||}$ values of 2.27–2.28 for Cu(II) complexes with an equatorial NO₃ coordination and $g_{||}$ values of 2.236 for an equatorial N₂O₂ geometry.⁵¹ Furthermore, the correlated ($g_{||}$, $A_{||}$) values agree with a NO₃ coordination for the first component (**3Si**) formed via condensation with one aminopropyl group and N₂O₂ surroundings for the second component (**2Si**), where reaction with two aminopropyl

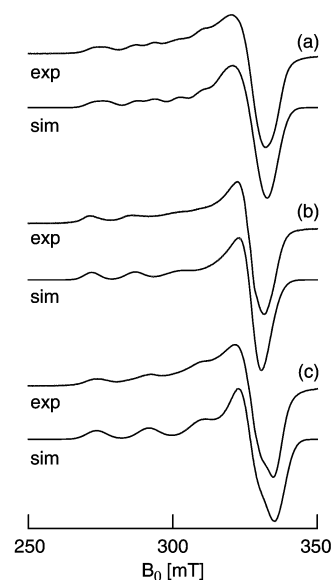


Figure 4. CW EPR spectra (exp = measured, sim = simulated) for immobilized **2Si** and **3Si** compounds. (a) Mixture of **2Si** and **3Si** (sample A), (b) **3Si** as the sole product at low aminopropyl modifier loading (sample B), and (c) recovered catalyst after leaching during an oxidation run, predominantly **2Si** (sample C). The simulation parameters can be found in Table 3.

groups has occurred.⁵⁰ The EPR parameters of **2Si** are similar to those for trans Cu(salicylaldehyde) complexes⁶⁰ and the silica aerogel-immobilized Cu(salenSi).¹⁵ This assignment is also in agreement with the fact that when lower aminopropyl loadings are used (sample B), only the **3Si** component remains, which has EPR parameters almost identical to those of the first component in sample A (Table 3). On the basis of simple calculations of the area and volume occupied by one aminopropyl group on the silica surface, it is not surprising that a double Schiff base reaction occurs at high (0.5 mmol g⁻¹ silica) aminopropyl modifier loading, providing a mixture of the NO₃ and N₂O₂ compounds on the surface. At lower aminopropyl loading (0.05 mmol g⁻¹ silica), only the NO₃ compound can form. Furthermore, the CW EPR spectrum of **3Si** (Figure 4b) shows larger g and A

(60) Jezowska-Trzebiatowska, B.; Jezierska, X. *J. Mol. Struct.* **1973**, *19*, 627.

strains (i.e., small local fluctuations in the direct surroundings of the Cu(II) ion lead to small differences in the g and A values for each **3Si** molecule), resulting in broader m_I -dependent line widths.⁶¹ In the case of lower loading, **3Si** is expected to have greater flexibility on the surface, and there will thus be a larger distribution of the molecular bonding parameters as compared with that for the product with higher aminopropyl loading on the silica surface. At relatively high aminopropyl loadings (1 mmol g⁻¹), reaction with **1** provides **2Si** as the major component (98%).

In the preceding paragraph, AP-SiO₂ was used as a functionalized support for the immobilization of **1** to provide **2Si** and **3Si** on the surface. Depending on the aminopropyl modifier loading, **2Si** or **3Si** is selectively prepared. At intermediate loadings, however, mixtures of **2Si** and **3Si** were always present on the surface. The immobilization of the homogeneous precursor **2** modified with pendant propyl-ethoxysilane groups on silica allows us to obviate this problem (Scheme 3). Using this approach, a single N₂O₂ component (**2Si**) is immobilized on silica for all loading levels. Alternatively, the reaction of **1** with triethoxysilyl-propylamine (2 equiv) provides the precursor **2**.

Figure 4c shows the CW EPR spectrum of the Cu(salenSi)-type material (sample C) following a catalytic allylic oxidation run in acetone/triethylamine (room temperature, under O₂, 1 bar).³⁶ Although the catalyst proved active, copper leaching from the matrix was confirmed by XPS analysis of the catalyst material before and after the run.³⁶ The EPR spectrum of C shows only one remaining component with the EPR parameters differing from those observed for sample A (i.e., the original catalyst material). The g and A^{Cu} values are, however, closer to those of **2Si** than those of **3Si**, and the (g_{\parallel} , A_{\parallel}) values agree with a N₂O₂ ligation for an uncharged complex.⁵⁰ The differences in the EPR parameters of sample C and **2Si** are probably due to triethylamine coordination at Cu(II). The broader line width observed in the CW EPR spectrum of sample C versus those of sample A is caused by the higher Cu(II) loading, which is necessary in catalysis. High local concentrations of copper are known to cause line broadening.⁶² This is an interesting but unwelcome example of preferential leaching during catalysis.³⁶ In an attempt to eliminate the copper leaching, the base component in the catalysis, triethylamine, was substituted by a silica-immobilized dimethylaminopropyl group.³⁶ The result was a stable but poor catalyst for allylic oxidation.

Early in our studies, the reaction of **1** with 1 equiv of γ -APS followed by immobilization on silica was investigated. The CW EPR of the immobilized product(s) (sample D) confirmed the presence of a mixture of **2Si** and **3Si** (52:48%) on the surface. This synthetic route was abandoned because it provided only a mixture of immobilization precursors. The CW EPR spectrum of copper acetate and salenHSiO₂ (sample E) on silica shows the contributions of two copper complexes (88:12%; Table 3 and Scheme 4). The first component is similar to the components described

already with NO₃ coordination at copper. Considering the reaction conditions (Scheme 4), in the absence of excess salicylaldehyde this component can be ascribed to the immobilized **4Si** molecule. The second component has EPR parameters identical to those found for copper acetate physically and chemically adsorbed on silica (Table 3, sample G). Comparison of the EPR spectrum of sample F, which represents the material recovered from the reaction of **3Si** with α -MBA, with the EPR data on **3Si** indicates that the reaction has not proceeded.

Davies-ENDOR and HYSCORE experiments have been conducted in order to corroborate the above interpretations of the CW EPR spectra. The samples used in the oxidation catalysis studies could not be measured using these techniques because of fast relaxation times arising from high copper concentrations (sample C). For copper acetate adsorbed on silica (sample G), no significant spin echoes could be observed as a result of the very low concentration of the complex in the matrix. All other samples were studied with pulse EPR and ENDOR. Figures 3b and 5a,b show the HYSCORE and Davies-ENDOR spectra, respectively, of sample D taken at observer position B (Figure 1a position corresponding to g_{\perp}). Because the two Cu(II) complexes **3Si** and **2Si** contribute to the CW EPR spectrum, these two complexes will also contribute to the pulse EPR and ENDOR spectra. When comparing parts b and a of Figure 3, we again recognize the presence of the cross peaks of the aldehyde protons and the ¹³C ridges, characteristic for the presence of a salicylaldehyde-type ligand. The presence of the aldehyde protons is confirmed by comparing the Davies-ENDOR spectra of sample D obtained with hard microwave pulses at two observer positions (parts b and d of Figure 5) with those of **1** in methanol/water at the same observer position (parts c and e of Figure 5). Although the total spectral width is retained, the proton hyperfine coupling in the latter case is slightly different from the one in the former case (see arrows). Our model study of **1** showed that the hyperfine coupling of the aldehyde protons did not depend on the matrix. The present observed change indicates that the salicylaldehyde-type ligand has been altered.

Furthermore, the ENDOR spectra of sample D show an additional broad peak in the 15–20 MHz region (parts b and d of Figure 5, signal marked with a square). At this frequency, no signal is observed in the HYSCORE spectra (see squares in Figure 3b), which indicates that it does not stem from a proton interaction. Because the signal was observed in the 15–20 MHz region for magnetic field settings throughout the whole EPR spectrum, it cannot be ascribed to the copper nucleus. We assign these peaks to directly coordinated nitrogens with signals centered around $a/2$. In a single-crystal ENDOR study of Cu(salicylaldimine) in Ni(salicylaldimine), nitrogen hyperfine interactions of $A_1 = 50.2$ MHz, $A_2 = 37.2$ MHz, and $A_3 = 39.1$ MHz have been observed.⁵⁵ Taking into account that the aldehyde proton couplings in Cu(salicylaldimine) were about 30% larger than those observed here and that this proton hyperfine coupling correlates with the unpaired electron density on the nitro-

(61) Froncisz, W.; Hyde, J. S. *J. Chem. Phys.* **1980**, *73*, 3123.

(62) Brüggeller, X.; Mayer, E. *Nature* **1980**, *288*, 569.

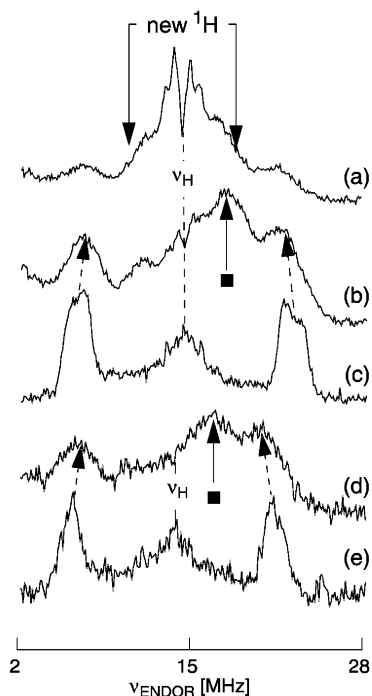


Figure 5. Davies-ENDOR spectra. Immobilized mixture of **2Si** and **3Si** (sample D) at observer position B with (a) weak pulses and (b) hard pulses. (c) **1** in methanol/water at observer position B (hard pulses). (d) Immobilized mixture of **2Si** and **3Si** (sample D) at observer position $B_0 = 316$ mT (hard pulses). (e) **1** in methanol/water at observer position $B_0 = 316$ mT (hard pulses).

gen,⁵⁵ a nitrogen hyperfine coupling of 30–40 MHz is reasonable for the immobilized **2Si**.

The Davies-ENDOR spectra of sample D obtained using weak microwave pulses differ clearly from those observed earlier for **1** in methanol/water (Figures 5a and 2a). This difference in the spectrum of the weakly coupled protons can also be appreciated from a comparison of the two HYSORE spectra in Figure 3 (region marked with new ^1H splitting). A new proton hyperfine interaction with a maximum splitting of about 8 MHz has appeared. An ENDOR study of Cu(II)-doped Ni(salicylaldimato) single crystals revealed for the ethylene protons hyperfine couplings up to 9.6 MHz.⁵⁵ The observation of these proton splittings thus again agrees with the presence of the propyl chain and confirms the reaction of the aminopropyl group with **1**. Furthermore, the hole in the ENDOR spectrum at the nuclear Zeeman frequency (Figure 5a) confirms that the Cu(II) complex is surrounded by silica. An ENDOR signal at ν_{H} arises mainly from remote matrix protons. Once the Cu(II) catalyst is mounted on the nonproton-containing matrix silica, this signal should decrease significantly, as is observed here. At the same time, a diagonal peak appears in the HYSORE spectrum at $(\nu_{\text{Si}}, \nu_{\text{Si}})$, which confirms the presence of ^{29}Si (thus silica) in the vicinity of the Cu(II) complexes (Figure 3b). Importantly, the absence of any signals of weakly coupled nitrogens in the HYSORE spectra rules out an axial coordination of Cu(II) by an aminopropyl group. The excellent solvating properties of DMSO, used as the solvent for the immobilization, may help to avoid formation of such an axial aminopropyl-coordinated **1** on the surface.^{21,22}

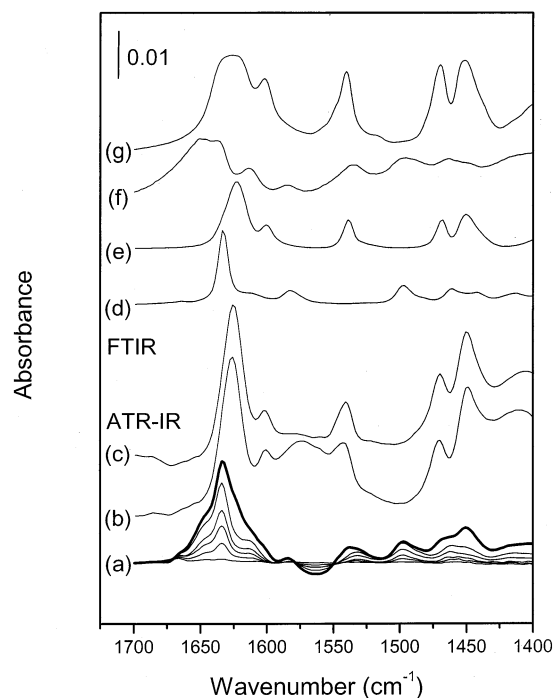


Figure 6. In situ ATR spectra of AP-SiO₂ on addition of (a) salicylaldehyde (step 1), (b) copper acetate hydrate (step 2) 10^{-3} M solutions in ethanol, and (c) neat-solvent flow. Flow times are 40, 10, and 30 min, respectively. For comparison, transmission IR spectra of neat (d) salenHSi and (e) **2Si** are included. Traces f and g show IR spectra of the KBr disks of materials as synthesized after steps 1 and 2, respectively. Traces in part a correspond to spectra recorded after 0.5, 2, 4, 12, and 40 min.

(D) In Situ ATR-IR Study of Cu(salenSi) Immobilization and Spectroscopic Characterization of Immobilized Compounds.

One of the immobilization approaches involves the reaction of salenHSi (1 mmol g^{-1}) immobilized on silica with a solution of copper acetate, providing **2Si** (Scheme 4). The metal loading can be controlled by the copper acetate concentration, reaction temperature, and reaction time. Step-wise synthesis of **2Si** on silica has been monitored in situ by ATR-IRS, and spectra in the range $1700\text{--}1400 \text{ cm}^{-1}$ are depicted in Figure 6a–c. Salicylaldehyde did not show significant adsorption on a SiO₂ film or on the bare IRE, so that the IR signals arise from the contact between salicylaldehyde and the aminopropyl groups. The strong signal at 1633 cm^{-1} , which increases in intensity on flowing a solution of salicylaldehyde over AP-SiO₂ (modifier loading 1 mmol g^{-1}) is attributed to the C=N stretching vibration of the immobilized salenHSi (Figure 6a).⁴⁴ Consequently, the negative-going band at about 1560 cm^{-1} (N–H) is associated with the decreasing concentration of the aminopropyl group as the reaction proceeds. The surface reaction of the aminopropyl groups with salicylaldehyde is instantaneous, as is observed in solution, and is only slowed down by the diffusion of the salicylaldehyde through the porous silica network. The weak signal at 1666 cm^{-1} , characteristic of salicylaldehyde [$\nu(\text{C}=\text{O})$], indicates that the IR radiation additionally samples the solution directly above the coated ATR crystal. This band disappears on admission of the copper acetate solution in the next step, suggesting the removal of salicylaldehyde from the solid–liquid interface,

whereas the peak maximum of the band at 1633 cm^{-1} is insensitive to neat-solvent flow. Signals occurring at about 760 and 740 cm^{-1} (not shown) are also associated with the formation of salenHSi on the modified silica surface. Inspection of the IR spectra of the precursor materials shows that these bands are characteristic of the metal complexes, in good agreement with data reported by Bigotto et al.⁶³ Furthermore, 4-methoxybenzaldehyde and 4-cyanobenzaldehyde were investigated to conclusively assign the signal at 1633 cm^{-1} to the $\nu(\text{C}=\text{N})$ of the immobilized imine group in step 1 (Scheme 4). Both substituted benzaldehydes exhibited a signal at 1645 cm^{-1} , which showed increasing intensity with reaction time. Moreover, a signal at 2229 cm^{-1} found for 4-cyanobenzaldehyde clearly indicated, together with that at 1645 cm^{-1} , the immobilization of the aromatic moiety, formation of the imine group, and presence of the $\text{C}\equiv\text{N}$ group on the SiO_2 surface.

Flowing a solution of copper acetate over the salenHSi-modified silica alters the ATR spectra (Figure 6b) as follows: the signal at 1633 cm^{-1} is red shifted to 1625 cm^{-1} with increased intensity and is attributed to formation of a surface-bound **2Si** (i.e., metal complexation).⁶⁴ Metal complexation perturbs the salicylaldehyde ring vibrations ($1650\text{--}1400\text{ cm}^{-1}$) by affecting the charge density and distribution, that is, band position and intensity. Upon coordination, the electronic contribution of the aromatic salicylalimine system to metal–ligand bonding is reflected in a decrease in frequency of these bands with new signals appearing at 1602 , 1540 , 1469 , and 1450 cm^{-1} . A similar effect has been observed for the ring vibrations of salicylic acid upon complexation with the Fe atoms of goethite.⁶⁴

The signals at about 1570 and 1410 cm^{-1} observed in trace b are associated with physisorbed copper acetate, which is readily removed by neat-solvent flow (Figure 6c). For comparison, copper acetate adsorption on the AP- SiO_2 surface was followed using the same concentration of copper acetate. Signals, enhanced by a factor of 6, were observed, indicating that the acetate readily adsorbs on silica. This clearly shows that if a ligand is present on the silica surface the adsorption of the acetate is less pronounced and metal coordination via the ligand is the dominant process. At lower loading (0.05 mmol g^{-1}), salenHSi reacts with copper acetate, showing IR signals characteristic of **4Si** (Scheme 4). Given the high copper acetate concentration used in the ATR-IR experiment, **4Si** is not observed at this aminopropyl loading due to the dominant signals of the adsorbed copper acetate.

Benzaldehydes absorb strongly in the region $1710\text{--}1685\text{ cm}^{-1}$ with internal hydrogen bonding, as in salicylaldehyde, reducing this signal to 1666 cm^{-1} .⁶⁵ Upon complexation, the $\text{C}=\text{O}$ band in salicylaldehyde is further reduced as in the M-bis(salicylaldehyde) complexes [1610 (Cu, **1**), 1627 (Co), and 1626 (Mn) cm^{-1}].^{37,38} The appearance of the characteristic stretching vibration of the newly formed $\text{C}=\text{N}$ bond

constitutes the most visible indicator of the reaction of free or coordinated $\text{C}=\text{O}$ in salicylaldehyde and M-bis(salicylaldehyde).⁶⁶ Bands characteristic of the salenHSi imine functionality are typically found in the range $1650\text{--}1590\text{ cm}^{-1}$ for the precursors and silica-incorporated compounds.^{9,15} For Cu(salenSi) precursors, the $\nu(\text{C}=\text{N})$ band appears at 1622 cm^{-1} . This band is found at 1625 cm^{-1} for the silica-gel-immobilized Cu(salenSi) and Cu(salenSi) aerogel.¹⁵ Although this provides information regarding the reaction outcome, alone it cannot be used as confirmation of the complex type on the surface.¹⁵

Discussion

1 has been used as a model to evaluate which EPR and ENDOR techniques were applicable for the characterization of immobilized Cu(salenSi)-type compounds. The results of the combined CW EPR, HYSCORE, and Davies-ENDOR experiments confirm the following points. CW EPR spectra show that two Cu(II) complexes are formed on the surface during the reaction of **1** with AP- SiO_2 (0.5 mmol g^{-1} modifier; Scheme 3; sample A in Table 3). The g and copper hyperfine values measured indicate that a different number of nitrogen atoms surround the copper in these two components and that equatorial NO_3 and *trans*- N_2O_2 coordination of the Cu(II) occurs. This is in agreement with a reaction where **1** reacts with one and two aminopropyl groups (Scheme 3). Davies-ENDOR and HYSCORE spectra of sample D confirm that for one of the two components on silica at least one nitrogen is coordinating to copper, hyperfine interactions compatible with the ones expected for the propyl protons are present, and a salicylaldehyde-type ligand is coordinating (i.e., presence of the aldehyde protons and the characteristic ^{13}C signals). Furthermore, the reduction of the ν_{H} signal in the Davies-ENDOR spectra and appearance of the ^{29}Si signal in the HYSCORE spectrum constitute strong evidence for immobilization on the silica surface.

The CW EPR spectrum of sample B (Table 3) contains only one component which is very similar to that of the second component (**3Si**) in sample A. The corresponding HYSCORE and Davies-ENDOR spectra of **3Si** (sample B) again reveal evidence of a reduced hyperfine splitting of the aldehyde proton, the presence of the propyl-type protons and nitrogens, and the presence of silicon in the vicinity of the copper complex. This proves that our initial assignment of NO_3 surroundings for this component in sample A on the basis of CW EPR is correct and that the second component (**2Si**) has N_2O_2 surroundings. In addition, the HYSCORE analyses show that neither of the two complexes undergo axial coordination with an aminopropyl group, which might have been expected on the basis of previous studies.^{21,22} Furthermore, the absence of any copper–copper interactions in the immobilized Cu(salenSi), such as those present in copper acetate, is confirmed.

We have applied ATR-IR to gain some insight into the stepwise modification of the silica surface with Cu(salenSi)

(63) Bigotto, A.; Reisenhofer, E.; Giordani, R. *Spectrochim. Acta* **1984**, *40A*, 203.

(64) Yost, E. C.; Tejedor-Tejedor, M. I.; Anderson, M. A. *Environ. Sci. Technol.* **1990**, *24*, 822.

(65) Lampert, H.; Mikenda, W.; Karpfen, A. *J. Phys. Chem. A* **1997**, *101*, 2254.

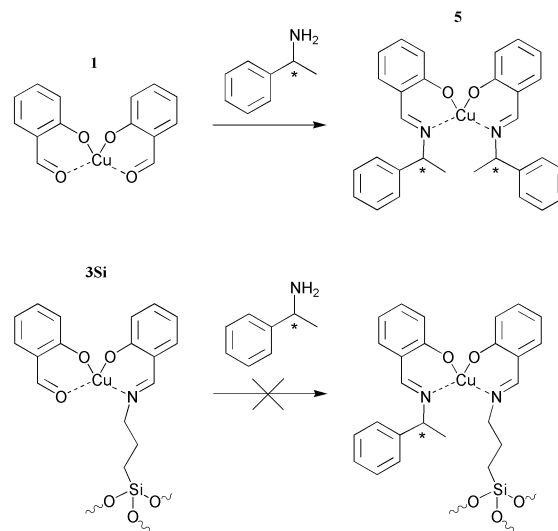
(66) Nakamoto, K. *Infrared and Raman Spectra of Inorganic and Coordination Compounds*; John Wiley & Sons: New York, 1997.

(Scheme 4 and Figure 6). To our knowledge, this is the first study on the immobilization of a metal center within a salen-ligand moiety using an in situ spectroscopic method in the presence of a solvent. Several additional features, including silica-copper acetate and silica-**1** interactions, are also detected using this method. A potential weakness of the ATR-IR technique in immobilization studies involving SiO₂-based materials lies in the background absorption of the support. Bands arising from the silica framework (Si-O-Si and Si-O vibrations in the 1250–900 cm⁻¹ spectral region) can mask useful information. For example, the signal centered at 1280 cm⁻¹, attributed to the phenolic C-O vibration of salicylaldehyde, appears with salenHSi formation (step 1, Scheme 4) and disappears when copper acetate is admitted to the salenHSi-modified silica film (step 2).⁹ Interference due to the strong Si-O-Si vibration of the silica thin film masks the new signal that is expected for this vibration.

In the past, the spectroscopic similarity of the precursors and aerogel-immobilized catalysts with structurally characterized compounds has often been used to confirm that the modified ligand also coordinates similarly.^{29–31} However, we have shown that for Cu(salenSi) the IR imine absorptions are insensitive to the N₂O₂ geometry (cis and trans) at the metal center, and EPR studies are necessary to confirm the precise coordination at the metal center.¹⁵ In addition, as the modifier loadings are reduced (e.g., 0.05 mmol g⁻¹), it becomes difficult to distinguish the corresponding bands. Convincing evidence of the structure of the immobilized complexes is, therefore, obtained only from combined EPR and IR studies.

On the basis of our combined EPR and in situ ATR-IR spectroscopic characterization of the precursors and immobilized materials, several facile synthetic routes to new heterogeneous systems with applications in oxidation catalysis have been elucidated. Our novel application of the Schiff base condensation enables facile immobilization of **1** on AP-SiO₂, providing immobilized salen-type catalysts (Scheme 3). To our knowledge, this approach has not been described in the literature to date. For salenSi-type systems, the reaction product on the surface can be controlled on the basis of the aminopropyl modifier loading. Such a strategy opens new synthetic routes to compounds not available by conventional synthetic procedures and enabled us to investigate the further modification of the metal-ligand system on the surface. Indeed, one of the main reasons that prompted this investigation was the possibility of introducing a chiral center at the unreacted carbonyl group in **3Si** on the silica surface, thereby opening an avenue to heterogeneous chiral Cu(salenSi) (Scheme 5). **1** reacts smoothly with α -MBA in solution, providing **5** (Scheme 5).^{23–28} Unfortunately, a comparable Schiff base condensation of **3Si** with α -MBA was not observed on the surface. On the basis of EPR studies of the recovered material, the coordination of α -MBA at copper is the dominant reaction (sample F, Table 3). Although unsuccessful, our simplified approach to the introduction of chirality would have obviated the laborious organic synthesis procedures described previously.³¹ Cur-

Scheme 5. Preparation Routes for Chiral Cu-bis(salicylaldehyde)-Type Homo- and Heterogeneous Complexes by Reaction of α -MBA with **1** and **3Si**



rently, we are investigating the reactions of chiral copper acetates (e.g., mandelates) with salenHSi immobilized on silica (Scheme 4) as a route to immobilized chiral half-salen copper catalysts.

Importance has been attached, in isolated cases, to the chain length of the spacer group used to chemically bind the catalyst and ligand to the support in relation to the catalytic activity.⁶⁷ The propyl group has been chosen here so as to avoid pore blockage while still retaining the flexibility of the ligand system. The flexibility of the propylamine spacer is clearly demonstrated in accommodating the Schiff base reaction of **1** with the silica-immobilized propylamine group, providing **2Si**. Furthermore, immobilized salenHSi on silica also accommodates the formation of Cu(salenSi) on the surface via the addition of a solution of a transition-metal salt (Scheme 4). An advantage of the above approach, that is, synthesis by the addition of a transition-metal salt, is that it offers some synthetic flexibility in catalyst development. Recently, a related stepwise approach has been used for the immobilization of a salicylaldehyde complex for epoxidation.³⁰ A complete characterization of the catalyst was not provided, and the proposed formulation as a half salenSi is unlikely on the basis of the salenSi and metal (6.8% by wt) loading. This high metal loading would suggest that the metal has, in fact, a N₂O₂ coordination.³⁰

Previously, direct interaction of the unmodified metal complex with the support during immobilization has not been considered an important factor. The adsorption of copper acetate hydrate (physical and chemical) from solution onto silica gel 100 shows that such a consideration may be significant in the absence of meticulous washing procedures. On the silica surface, copper acetate is coordinated by four oxygens in a highly strained geometry (sample G, Table 3). Similarly, **1** adsorbs on silica via two modes, as evidenced by EPR. Interestingly, such M-O interactions have been

(67) Hartley, E. R. *Catalysis by Metal Complexes, Supported Metal Reagents*; D. Reidel: Dordrecht, Germany, 1984.

Cu(salicylaldimine)

reported for Cu(salicylaldimine) in the cages of zeolite Y, where treatment of the Cu(salicylaldimine) with acetonitrile was accompanied by a green-to-red color change and significant change in catalytic activity.¹¹

Conclusions

Using a combination of EPR and IR spectroscopies, we are able to confirm our synthetic findings and make the following conclusions. The novel application of the familiar Schiff base condensation enables facile immobilization of Cu-bis(salicylaldehyde) precursors on AP-SiO₂. In addition, the Schiff base reaction provides a very useful tool in the stepwise immobilization of Cu(salicylaldimine) compounds. Importantly, the synthesis of compounds not available by

conventional synthetic procedures is possible via the surface-synthesis strategy. Utilizing mesoporous silica as the support obviates the sol-gel procedure and scCO₂ drying necessary to produce silica aerogels. Finally, the relevance of N-containing ligands for homogeneous and heterogeneous catalysis is considerable, and it is expected that future studies centered on the catalytic behavior of the immobilized compounds for oxidation catalysis will provide interesting results.

Acknowledgment. The authors wish to thank Dr. Thomas Bürgi for invaluable XPS measurements and Dr. Marek Maciejewski for thermal analysis.

IC020298P